GEOPHYSICS, VOL. 54, NO. 7 (JULY 1989); P. 921–926, 3 FIGS.

Short Note

Backprojection versus backpropagation in multidimensional linearized inversion

Cengiz Esmersoy* and Douglas Miller*

INTRODUCTION

Seismic migration can be viewed as either backprojection (diffraction-stack) or backpropagation (wave-field extrapolation) (e.g., Gazdag and Sguazzero, 1984). Migration by backprojection was the view supporting the first digital methods—the diffraction and common tangent stacks of what is now called classical or statistical migration (Lindsey and Hermann, 1970; Rockwell, 1971; Schneider, 1971; Johnson and French, 1982). In this approach, each data point is associated with an isochron surface passing through the scattering object. Data values are then interpreted as projections of reflectivity over the associated isochrons. Dually, each image point is associated with a reflection-time surface passing through the data traces. The migrated image at that point is obtained as a weighted stack of data lying on the reflection-time surface (Rockwell, 1971; Schneider, 1971). This amounts to a weighted backprojection in which each data point contributes to image points lying on its associated isochron.

With the introduction of wave-equation methods by Claerbout (1971), this backprojection view was largely replaced by a backpropagation approach in which the recorded waves are extrapolated either downward in space or backward in time and the image extracted from the extrapolated wave field by an imaging condition (e.g., Berkhout, 1984; Stolt and Weglein, 1985). In the case of a single-source, multiple-receiver experiment, the simplest imaging condition consists of reading the value of the extrapolated field at each image point at the time of illumination from the source. This reverse propagation constitutes the solution of a boundary-value problem and can be accomplished either by means of a finite-difference simulation constrained by data values along the receiver array (Whitmore, 1983; Baysal et al., 1983; Chang and McMechan, 1986; Whitmore and Lines, 1986) or by means of a Kirchhoff integral (Schneider, 1978; Wiggins, 1984). The Kirchhoff formulation provides a key to the reconciliation of backprojection migration with the wave equation. It is formulated in terms of the backpropagation approach, but implemented as a backprojection. In this way one obtains the weights and prefiltering operations that are required to make the two algorithms equivalent.

Recently, these classical migration methods have been reformulated in terms of a theory of multidimensional linearized inversion (Born inversion). Within this theory, the seismic imaging problem is recast from that of extrapolating a scattered wave field to one of recovering the perturbations of material parameters (the scattering potential) that gave rise to the scattered field. As with the earlier methods, multidimensional Born inversion can be formulated either in terms of backprojection (Miller et al., 1984; Beylkin, 1985; Miller et al., 1987) or (for certain experimental geometries) in terms of backpropagation (Cheng and Coen, 1984; Esmersoy, 1986; Esmersoy and Oristaglio, 1988). For the case of zero-offset geometry, the two inversion formulas agree in the far field and differ from classical wave-equation migration only by a one-dimensional filter which is applied to the data traces before backprojection or backpropagation (Jakubowicz and Miller, 1989). For a single-source, multiple-receiver geometry, backprojection inversion differs from standard backprojection migration by adding to the integrand an extra "obliquity factor" that depends on the angle between the source and receiver rays at each image point. The backpropagation inversion method (Esmersoy, 1986; Esmersoy and Oristaglio, 1988) differs from standard backpropagation migration by adding an extra spatial differential operator which is applied to the extrapolated wave field before imaging.

In this note, we discuss the relationship between these two formulations of single-source migration. We show that the two linearized methods satisfy the same formal equivalence as the earlier methods. In particular, the extra stacking weights applied in backprojection inversion are identical to

Manuscript received by the Editor October 22, 1987; revised manuscript received September 12, 1988.
*Schlumberger-Doll Research, Old Quarry Road, Ridgefield, CT 06877-4108.

the weights applied implicitly to the plane-wave components in backpropagation inversion. If the source and receivers are in the far field of the imaging region, these two methods give the same result.

THE BASIC RELATION

As described above, backprojection imaging is implemented as an integral over the receiver data, whereas backpropagation imaging is obtained by a local operation inside the scattering medium after the data are extrapolated from the receivers into the medium by using a finite-difference algorithm, Kirchhoff integral, or frequency-wavenumber technique. It appears difficult, therefore, to make a term-by-term comparison of these methods. However, a direct relation becomes evident when we consider how these methods reconstruct local spatial projections at each point in the migrated image.

In the backprojection formulation, each data point represents the integral of reflectivity over an isochron curve (an ellipse in the case of a homogeneous background). For a given image point, data points on the reflection-time curve are associated with integrals along isochron curves passing through the image point. In the vicinity of the image point, these isochron curves can be approximated by straight lines (Miller et al., 1987). Thereby, each receiver data point is locally associated with a line integral through the image point (see Figure 1).

In the backpropagation formulation the counterpart of the above discussion is as follows: When a medium is probed by a plane-wave source, the plane-wave components of the *scattered* field are directly related to straight-line integrals of reflectivity (e.g., Esmersoy and Levy, 1986). In the case of a point source, we can assume that the incident field has a locally plane wavefront in the vicinity of an image point. Then, each plane-wave component of the *backpropagated* field at the image point is associated with a line integral through the point (see Figure 2).

Thus, a given spatial projection (line integral) is locally associated either with an individual receiver datum in the backprojection formulation or with an individual plane-wave component of the backpropagated field. It is seen from the above discussion that, functionally, receiver data in the backprojection formulation correspond to the plane-wave components of the field in the backpropagation formulation. In what follows, this relation is shown more explicitly. For concreteness we work with algorithms formulated for 2-D acoustic propagation in models with constant density and variable velocity.

COMPARISON OF INVERSION INTEGRALS

The backprojection form of the 2-D single-source inversion derived from consideration of the generalized Radon transform is given in Miller et al. [equation (27a), 1987]. The reconstructed scattering potential f_S is written

$$f_S = -\frac{s_0^2}{\pi a_S}\int d\hat{\mathbf{u}}\,\cos^2\alpha\,\frac{1}{a_R}\,\mathcal{H}p_s(\mathbf{r}_R,\, t=\tau_S+\tau_R), \qquad (1)$$

where p_s is the scattered field trace, s_0 is the background slowness, $\hat{\mathbf{u}}$ is the unit vector along the ray connecting image point $\mathbf{r}$ to receiver $\mathbf{r}_R$ (see Figure 1), and $\mathcal{H}$ denotes Hilbert transform in time. τ and a denote the traveltime and geometrical spreading between the image point and the source (with index S) or receiver (with index R). The angle α is half of the angle between the source and receiver rays at the image point as shown in Figure 1.

In backpropagation migration, "imaging" the backpropagated field by using some imaging principle implicitly results in a weighted superposition of the plane-wave components of the backpropagated field at the image point. As shown in Appendix A, the basic inversion formula of Esmersoy and Oristaglio (1988) can be written

$$f_R(\mathbf{r}) = \frac{2s_0^2}{a_S}\left\{\frac{1}{s_0^2}\,\nabla\tau_S\cdot\nabla+\frac{\partial}{\partial t}\right\}\mathcal{F}p_e(\mathbf{r},\, t=\tau_S), \qquad (2)$$

where f_R is the reconstructed scattering potential, p_e is the backpropagated field, $\mathcal{F}$ is a filter with frequency response $(i\omega)^{-1}(-i\omega)^{-1/2}$, and ∇ denotes gradient with respect to $\mathbf{r}$. Note that the differential operator inside the braces is a one-way wave operator along the rays of the incident source field. The

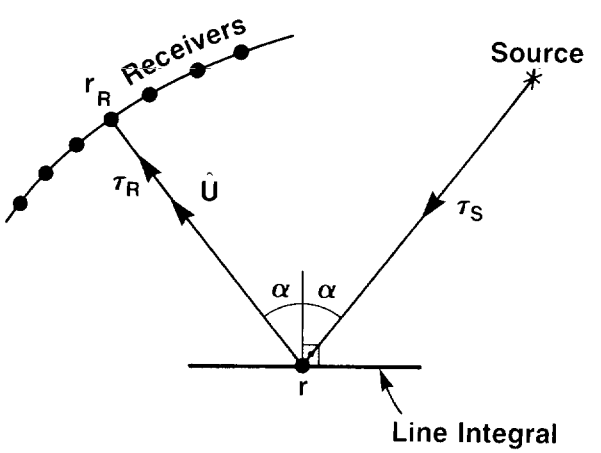

FIG. 1. In backprojection migration, the data points $\tau_S + \tau_R$ of each receiver give a line integral passing through the image point.

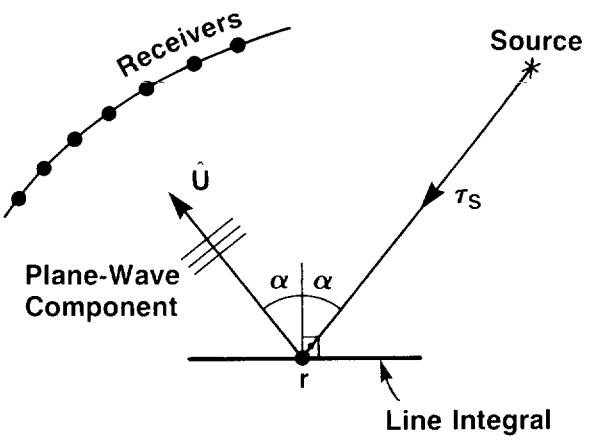

FIG. 2. In backpropagation migration, the data point $\tau_S - s_0\hat{\mathbf{u}}\cdot\mathbf{r}$ of each plane-wave component gives a line integral passing through the image point; s_0 is the background slowness.

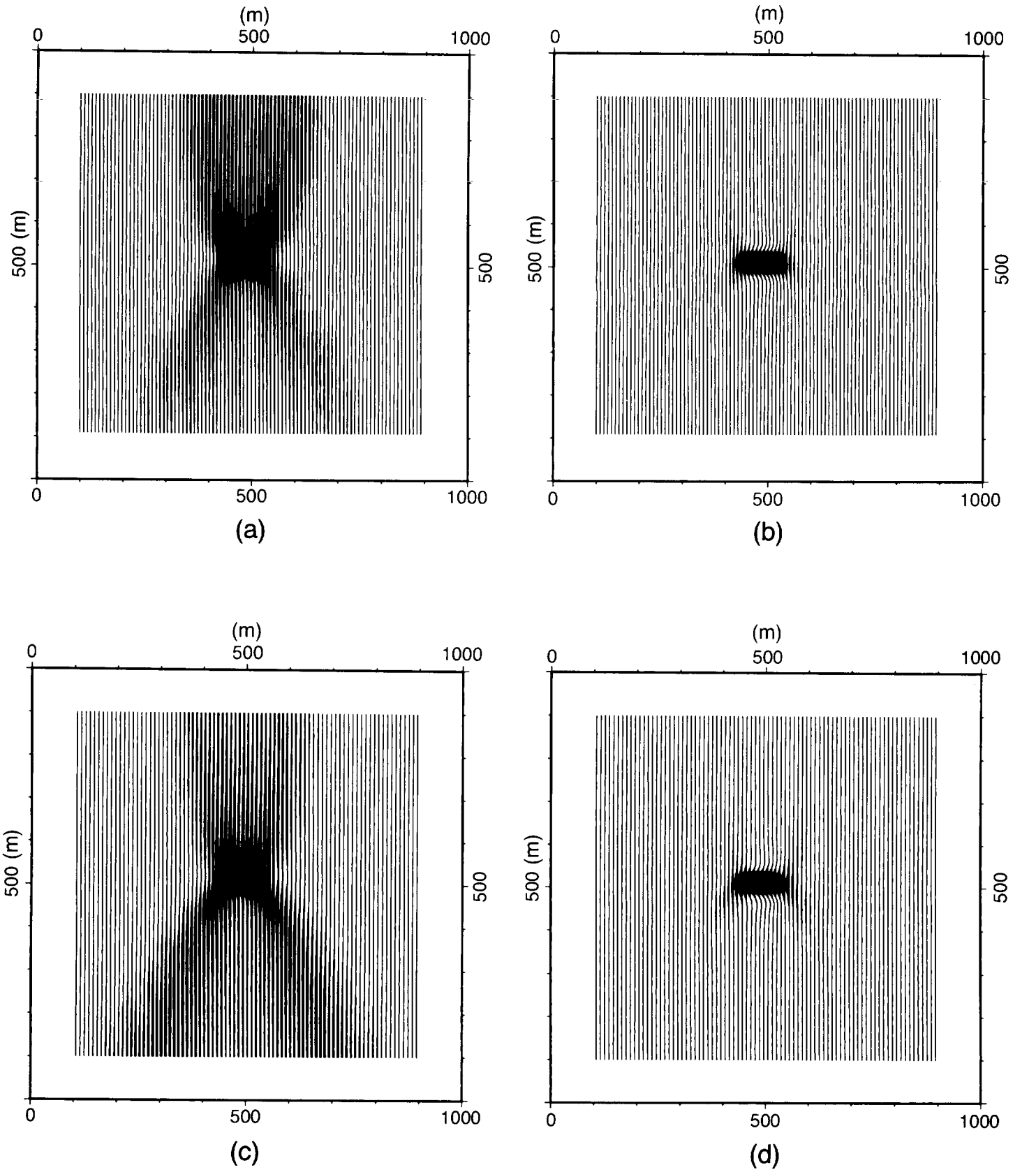

FIG. 3. Single-source, multireceiver point reconstructions using (a) backprojection, (b) refined backprojection, (c) backpropagation, and (d) refined backpropagation. The source was a 40 Hz Blackman-Harris pulse located at $x = 500$ m (horizontal axis), $z = -500$ m (vertical axis). Receivers were located on the frame completely surrounding the images with a uniform 20 m spacing. The medium consisted of a point velocity anomaly at $x = z = 500$ m (1000 m below the source) in a homogeneous medium with velocity 10 000 m/s. Traces were obtained by means of a finite-difference simulation.

backpropagated field p_e can be viewed as the superposition of the backpropagated plane-wave components of the scattered field. Let $q(\hat{\mathbf{u}}, t)$ be the plane-wave component of the scattered field along the direction $\hat{\mathbf{u}}$ (see Figure 2). Backpropagation of a plane-wave component to a given point is accomplished by a simple time-shift operation. More precisely, the plane-wave component $\hat{\mathbf{u}}$ backpropagated to a point $\mathbf{r}$ is given by $q(\hat{\mathbf{u}}, t - s_0\hat{\mathbf{u}} \cdot \mathbf{r})$. It is shown in Appendix B that the backpropagated field satisfies the relation

$$p_e(\mathbf{r}, t) = \frac{1}{4\pi}\int d\hat{\mathbf{u}}\ \mathcal{H}q(\hat{\mathbf{u}}, t - s_0\hat{\mathbf{u}} \cdot \mathbf{r}). \tag{3}$$

From equations (2) and (3),

$$f_R(\mathbf{r}) = \frac{s_0^2}{\pi a_S}\int d\hat{\mathbf{u}}\ \frac{1}{2}\left\{\frac{1}{s_0^2}\nabla\tau_S \cdot \nabla + \frac{\partial}{\partial t}\right\}\mathcal{H}\mathcal{F}q(\hat{\mathbf{u}}, t - s_0\hat{\mathbf{u}} \cdot \mathbf{r}). \tag{4}$$

Due to the form of the second argument of q, the gradient operation can be replaced by $-s_0\hat{\mathbf{u}}(\partial/\partial t)$. Then,

$$f_R(\mathbf{r}) = \frac{s_0^2}{\pi a_S}\int d\hat{\mathbf{u}}\ \frac{1}{2}\left[-\frac{1}{s_0}\nabla\tau_S \cdot \hat{\mathbf{u}} + 1\right]\frac{\partial}{\partial t}\mathcal{H}\mathcal{F}q(\hat{\mathbf{u}}, t - s_0\hat{\mathbf{u}} \cdot \mathbf{r}). \tag{5}$$

Here, $(1/s_0)\nabla\tau_S$ is the unit vector tangent to the source ray at the image point $\mathbf{r}$. Thus, half of the bracketed term in equation (5) can be written as

$$\frac{1}{2}\left[-\frac{1}{s_0}\nabla\tau_S \cdot \hat{\mathbf{u}} + 1\right] = \frac{1}{2}(\cos 2\alpha + 1) = \cos^2\alpha, \tag{6}$$

where 2α is the angle between the source ray and the plane-wave direction.

Finally, from equations (5) and (6) and by defining the filter $\mathcal{G} = -(\partial/\partial t)\mathcal{F}$, we have an explicit expression for the migrated image as a weighted superposition of plane waves

$$f_R(\mathbf{r}) = -\frac{s_0^2}{\pi a_S}\int d\hat{\mathbf{u}}\ \cos^2\alpha\ \mathcal{H}\mathcal{G}q(\hat{\mathbf{u}}, t = \tau_S - s_0\hat{\mathbf{u}} \cdot \mathbf{r}), \tag{7}$$

where $\mathcal{G}$ is a filter with frequency response $(-i\omega)^{-1/2}$.

The correspondence between equations (1) and (7) is now evident. Specifically, the filtered plane-wave components $\mathcal{G}q(\hat{\mathbf{u}}, t)$ in equation (7) are replaced by the scaled scattered field $p_s(\mathbf{r}_R, t)/a_R$ in equation (1). The receiver location $\mathbf{r}_R$ is the intersection of the receiver array with the ray defined by $\hat{\mathbf{u}}$ at the image point. In fact, we can pass directly from equation (1) to equation (7) (and vice versa) by substituting from the *far-field* expression of p_s in terms of q (stated here in terms of Fourier transforms):

$$P_s(\mathbf{r}_R, \omega) \approx (-i\omega)^{-1/2}a_R \exp[i\omega(\tau_R + s_0\hat{\mathbf{u}} \cdot \mathbf{r})]Q(\hat{\mathbf{u}}, \omega). \tag{8}$$

This relation is formally derived in Appendix C. It reflects the well-known fact in scattering theory that if we take a receiver to infinity along some direction $\hat{\mathbf{u}}$, then the observed scattered field asymptotically becomes identical to the filtered plane wave in that direction. Consequently, if the receiver array is far from the reflector being imaged, then the backprojection inversion f_S and the backpropagation inversion f_R become the same.

COMPARISON OF POINT IMAGES

In order to illustrate the relationship between the two methods, in Figure 3 we show migrated images of a point scatterer obtained by backprojection and backpropagation algorithms.

Figures 3a and 3b show point images obtained by backprojection migration and inversion, respectively. In both cases, traces were Hilbert transformed in time before stacking. The difference between these two reconstructions is the obliquity factor [$\cos^2\alpha$ in equation (1)], which is absent in migration. Figures 3c and 3d show point images obtained by backpropagation migration and inversion, respectively. Backpropagation is implemented by using a reverse-time finite-difference algorithm. Again, in both cases, traces were prefiltered so that the only difference between these two images is the implicit weighting factor [$\cos^2\alpha$ in equation (7)], which is absent in migration. Note that straightforward 2-D reverse-time migration (e.g., Chang and McMechan, 1986) does not include the temporal prefilter which is used here. More detailed analysis of backpropagation migration algorithms can be found in Esmersoy and Oristaglio (1988). Although this example with receivers below the anomaly is not realistic, it shows that, for either method, the obliquity factor clearly has a much larger effect than that due to the difference between the backprojection and backpropagation approaches.

CONCLUSION

2-D backprojection and backpropagation migration algorithms can be viewed as reconstructions of scattering objects from their line integrals. In backprojection, these line integrals are associated with data points of the scattered field; in backpropagation, they are associated with the plane-wave components of the scattered field. In both algorithms, image points are reconstructed by weighted sums of the corresponding line integrals. A quantitative comparison of two recent algorithms shows that the stacking weights in backprojection inversion are the same as the weights implicitly applied to the plane-wave components in backpropagation inversion.

REFERENCES

Baysal, K., Kosloff, D. D., and Sherwood, J. W. C., 1983, Reverse-time migration: Geophysics, **48**, 1514–1524.

Berkhout, A. J., 1984, Multidimensional linearized inversion and seismic migration: Geophysics, **49**, 1881–1895.

Beylkin, G., 1985, Imaging of discontinuities in the inverse scattering problem by inversion of a causal generalized Radon transform: J. Math. Phys., **26**, 99–108.

Chang, W., and McMechan, G. A., 1986, Reverse-time migration of offset vertical seismic profiling data using the excitation-time imaging condition: Geophysics, **51**, 67–84.

Cheng, G., and Coen, S. 1984, The relationship between Born inversion and migration for common-midpoint stacked data: Geophysics, **49**, 2117–2131.

Claerbout, J. F., 1971, Toward a unified theory of reflector mapping: Geophysics, **36**, 467–481.

Esmersoy, C., and Levy, B. C., 1986, Multidimensional Born inversion with a wide-band plane-wave source: Proc. IEEE, **74**, 466–475.

Esmersoy, C., 1986, Inversion by reverse-time extrapolation and a new imaging principle: 56th Ann. Internat. Mtg., Soc. Expl. Geophys., Expanded abstracts, 608–611.

Esmersoy, C., and Oristaglio, M. L., 1988, Reverse-time wave-field extrapolation, imaging, and inversion: Geophysics, **53**, 920–931.

Gazdag, J., and Sguazzero, P., 1984, Migration of seismic data: Proc. IEEE, **72**, 1302–1315.

Jakubowicz, H., and Miller, D., 1989, Two-pass 3-D migration and inversion in the (x, t) domain: Geophys. Prosp., **37**, 143–148.

Johnson, J. D., and French, W. S., 1982, Migration—The inverse

method, *in* Jain, K. C., and deFigueiredo, R. J. P., Eds., Concepts and techniques in oil and gas exploration: Soc. Expl. Geophys.
Lindsey, J. P., and Hermann, A., 1970, Digital migration: Oil and Gas Jour., **68**, Feb. 16, 112–115.
Miller, D., Oristaglio, M., and Beylkin, G., 1984, A new formalism and an old heuristic for seismic migration: 54th Ann. Internat. Mtg., Soc. Expl. Geophys., Expanded abstracts, 704–707.
———1987, A new slant on seismic imaging: Classical migration and integral geometry: Geophysics, **52**, 943–964.
Rockwell, D. W., 1971, Migration stack aids interpretation: Oil and Gas J., **69**, Apr. 19, 202–218.
Schneider, W. A., 1971, Developments in seismic data processing and analysis (1968–1970): Geophysics, **36**, 1043–1073.
———1978, Integral formulation for migration in two and three dimensions: Geophysics, **43**, 49–76.
Stolt, R. H., and Weglein, A. B., 1985, Migration and inversion of seismic data: Geophysics, **50**, 2458–2472.
Whitmore, D., 1983, Iterative depth migration by backward time propagation: 53rd Ann. Internat. Mtg., Soc. Expl. Geophys., Expanded abstracts, 382–385.
Whitmore, N. D., and Lines, L. R., 1986, Vertical seismic profiling depth migration of a salt dome flank: Geophysics, **51**, 1087–1109.
Wiggins, J. W., 1984, Kirchhoff integral extrapolation and migration of nonplanar data: Geophysics, **49**, 1239–1248.

APPENDIX A

DERIVATION OF EQUATION (2)

In Esmersoy (1986) and Esmersoy and Oristaglio (1988), the reconstructed image f_R is defined in the frequency domain. In the following, we derive the equivalent time-domain expression. From equation (23) in Esmersoy and Oristaglio (1988),

$$f_R(\mathbf{r}) = \frac{1}{2\pi}\int_{-\infty}^{\infty} d\omega\, \frac{F(\omega)\mathcal{L}_0(\mathbf{r}, \omega)P_c(\mathbf{r}, \omega)}{P_0(\mathbf{r}, \omega)}, \qquad \text{(A-1)}$$

where P_c is the backpropagated field,

$$F(\omega) = 2/\omega^2, \qquad \text{(A-2)}$$

$$\mathcal{L}_0(\mathbf{r}, \omega) = \{\nabla\tau_S \cdot \nabla - s_0^2 i\omega\}, \qquad \text{(A-3)}$$

and incident field P_0 for an impulse source is

$$P_0(\mathbf{r}, \omega) = (-i\omega)^{-1/2} a_S e^{i\omega\tau_S}. \qquad \text{(A-4)}$$

Using equations (A-2), (A-3), and (A-4) in equation (A-1), we obtain

$$f_R(\mathbf{r}) = \frac{2}{a_S}\frac{s_0^2}{2\pi}\int_{-\infty}^{\infty} d\omega \left\{\frac{1}{s_0^2}\nabla\tau_S \cdot \nabla - i\omega\right\} \frac{P_c(\mathbf{r}, \omega)}{i\omega(-i\omega)^{1/2}} e^{-i\omega\tau_S}. \qquad \text{(A-5)}$$

Equation (A-5), viewed as an inverse Fourier transform, gives equation (2), where p_c is the inverse transform of P_c and $\mathcal{F}$ is a filter with frequency response $(i\omega)^{-1}(-i\omega)^{-1/2}$.

APPENDIX B

DERIVATION OF EQUATION (3)

In Esmersoy and Levy (1986), the plane-wave components are explicitly defined in terms of the scattered field by equation (7), where $Q(\hat{\mathbf{u}}, \omega)$ is the Fourier transform of $q(\hat{\mathbf{u}}, t)$. Following the Appendix of that paper, setting $S(\omega)=1$ (for an impulse source), replacing $s_0^2\gamma(\mathbf{r})$ by $f(\mathbf{r})$ and $e^{i\mathbf{k}_i\cdot\mathbf{r}}$ by $P(\mathbf{r}, \omega)$ (for an arbitrary excitation instead of a plane-wave source), we have

$$Q(\hat{\mathbf{u}}, \omega) = \omega^2 \int_V d\mathbf{r}' f(\mathbf{r}')P(\mathbf{r}', \omega) \exp(-i\omega s_0 \hat{\mathbf{u}} \cdot \mathbf{r}'), \qquad \text{(B-1)}$$

where V denotes the volume containing the scatterers. From equations (5) and (7) in Esmersoy and Oristaglio (1988), the extrapolated field can be written as

$$P_c(\mathbf{r}, \omega) = \frac{i\,\mathrm{sgn}(\omega)\omega^2}{4\pi} \int d\hat{\mathbf{u}} \exp(i\omega s_0 \hat{\mathbf{u}}\cdot\mathbf{r}') \times \int_V d\mathbf{r}' f(\mathbf{r}')P(\mathbf{r}', \omega) \exp(-i\omega s_0 \hat{\mathbf{u}}\cdot\mathbf{r}). \qquad \text{(B-2)}$$

Using equation (B-1) in equation (B-2), we obtain

$$P_c(\mathbf{r}, \omega) = \frac{1}{4\pi}\int d\hat{\mathbf{u}}\, i\,\mathrm{sgn}(\omega) Q(\hat{\mathbf{u}}, \omega) \exp(i\omega s_0 \hat{\mathbf{u}}\cdot\mathbf{r}). \qquad \text{(B-3)}$$

An inverse Fourier transform of both sides gives equation (3).

APPENDIX C

DERIVATION OF EQUATION (8)

The scattered field, observed at an arbitrary point $\mathbf{r}_R$, is given by the volume integral [e.g., Esmersoy and Oristaglio (1988), equation (4)]

$$P_s(\mathbf{r}_R, \omega) = \omega^2 \int_V d\mathbf{r}' f(\mathbf{r}')P(\mathbf{r}', \omega)G_0(\mathbf{r}_R, \mathbf{r}', \omega), \qquad \text{(C-1)}$$

where G_0 is the background Green's function and V is the bounded support of the scatterers. For a homogeneous background and at large distances from the scattering volume (i.e., $\omega s_0|\mathbf{r}_R - \mathbf{r}'| \gg 1$, for all $\mathbf{r}' \in V$ and the origin of the coordinates is chosen in the neighborhood of V), the Green's function can be approximated

$$G_0(\mathbf{r}_R, \mathbf{r}', \omega) \approx (-i\omega)^{-1/2} a_R \exp(i\omega s_0 |\mathbf{r}_R - \mathbf{r}'|), \qquad \text{(C-2)}$$

where $a_R = (8\pi s_0|\mathbf{r}_R - \mathbf{r}'|)^{-1/2}$ is the geometric spreading term.

Now consider the following identity:

$$\begin{aligned}|\mathbf{r}_R - \mathbf{r}'| &= [(\mathbf{r}_R - \mathbf{r}') \cdot (\mathbf{r}_R - \mathbf{r}')]^{1/2} \\ &= [|\mathbf{r}_R|^2 - 2\mathbf{r}_R \cdot \mathbf{r}' + |\mathbf{r}'|^2]^{1/2} \\ &= |\mathbf{r}_R| \left[1 - 2\frac{\hat{\mathbf{r}}_R \cdot \mathbf{r}'}{|\mathbf{r}_R|} + \frac{|\mathbf{r}'|^2}{|\mathbf{r}_R|^2}\right]^{1/2}, \end{aligned} \tag{C-3}$$

where $\hat{\mathbf{r}}_R = \mathbf{r}_R/|\mathbf{r}_R|$ is the unit vector pointing to the receiver. For $|\mathbf{r}_R| \to \infty$, by keeping only the first-order terms, we have

$$|\mathbf{r}_R - \mathbf{r}'| \approx |\mathbf{r}_R| \left[1 - 2\frac{\hat{\mathbf{r}}_R \cdot \mathbf{r}'}{|\mathbf{r}_R|}\right]^{1/2}. \tag{C-4}$$

The first-order Taylor expansion of the square root gives

$$\begin{aligned}|\mathbf{r}_R - \mathbf{r}'| &\approx |\mathbf{r}_R| \left[1 - \frac{\hat{\mathbf{r}}_R \cdot \mathbf{r}'}{|\mathbf{r}_R|}\right] \\ &= |\mathbf{r}_R| - \hat{\mathbf{r}}_R \cdot \mathbf{r}', \end{aligned} \tag{C-5}$$

and

$$\begin{aligned}|\mathbf{r}_R - \mathbf{r}'|^{1/2} &\approx |\mathbf{r}_R|^{1/2} \left[1 - \frac{\hat{\mathbf{r}}_R \cdot \mathbf{r}'}{2|\mathbf{r}_R|}\right] \\ &\approx |\mathbf{r}_R|^{1/2}. \end{aligned} \tag{C-6}$$

From equations (C-1), (C-2), and (C-5),

$$\begin{aligned}P_s(\mathbf{r}_R, \omega) \approx (-i\omega)^{-1/2} a_R \exp(i\omega s_0 |\mathbf{r}_R|)\, \omega^2 \\ \times \int_V d\mathbf{r}'\, f(\mathbf{r}') P(\mathbf{r}', \omega) \\ \times \exp(-i\omega s_0 \hat{\mathbf{r}}_R \cdot \mathbf{r}'), \end{aligned} \tag{C-7}$$

and using equation (B-1), we obtain the relation

$$P_s(\mathbf{r}_R, \omega) \approx (-i\omega)^{-1/2} a_R \exp(i\omega s_0 |\mathbf{r}_R|)\, Q(\hat{\mathbf{r}}_R, \omega). \tag{C-8}$$

Finally, by shifting the origin to an arbitrary point $-\mathbf{r}$, we obtain equation (8), where $\tau_R = s_0|\mathbf{r}_R - \mathbf{r}|$ and $\hat{\mathbf{u}} = (\mathbf{r}_R - \mathbf{r})/|\mathbf{r}_R - \mathbf{r}|$.